

論文 / 著書情報  
Article / Book Information

Title	Secondary Resonance Magnetic Force Microscopy
Authors	Suguru Tanaka, Yasuo Azuma, YUTAKA MAJIMA
Citation	J. Appl. Phys., Vol. 111, ,
発行日/Pub. date	2012, 4
公式ホームページ /Journal home page	<a href="http://jap.aip.org/">http://jap.aip.org/</a>
権利情報/Copyright	Copyright (c) 2012 American Institute of Physics

## Secondary resonance magnetic force microscopy

Suguru Tanaka, Yasuo Azuma, and Yutaka Majima

Citation: *J. Appl. Phys.* **111**, 084312 (2012); doi: 10.1063/1.4705400

View online: <http://dx.doi.org/10.1063/1.4705400>

View Table of Contents: <http://jap.aip.org/resource/1/JAPIAU/v111/i8>

Published by the [American Institute of Physics](#).

---

### Related Articles

High resolution switching magnetization magnetic force microscopy  
*Appl. Phys. Lett.* **102**, 062405 (2013)

Nanoparticles charge response from electrostatic force microscopy  
*Appl. Phys. Lett.* **102**, 053118 (2013)

Tip-induced artifacts in magnetic force microscopy images  
*Appl. Phys. Lett.* **102**, 022417 (2013)

High aspect ratio nanoneedle probes with an integrated electrode at the tip apex  
*Rev. Sci. Instrum.* **83**, 113704 (2012)

Rapid preparation of electron beam induced deposition Co magnetic force microscopy tips with 10 nm spatial resolution  
*Rev. Sci. Instrum.* **83**, 093711 (2012)

---

### Additional information on *J. Appl. Phys.*

Journal Homepage: <http://jap.aip.org/>

Journal Information: [http://jap.aip.org/about/about\\_the\\_journal](http://jap.aip.org/about/about_the_journal)

Top downloads: [http://jap.aip.org/features/most\\_downloaded](http://jap.aip.org/features/most_downloaded)

Information for Authors: <http://jap.aip.org/authors>

## ADVERTISEMENT



**AIP Advances**

Now Indexed in  
Thomson Reuters  
Databases

Explore AIP's open access journal:

- Rapid publication
- Article-level metrics
- Post-publication rating and commenting

## Secondary resonance magnetic force microscopy

Suguru Tanaka,<sup>1</sup> Yasuo Azuma,<sup>1</sup> and Yutaka Majima<sup>1,2,a)</sup><sup>1</sup>Materials and Structures Laboratory, Tokyo Institute of Technology, Yokohama 226-8503, Japan<sup>2</sup>Department of Printed Electronics Engineering, Sunchon National University, Sunchon 540-742, Korea

(Received 22 February 2012; accepted 23 March 2012; published online 23 April 2012)

In this study, we have developed secondary resonance magnetic force microscopy (SR-MFM) for imaging alternating magnetic fields from a sample surface at the secondary resonant frequency of the magnetic cantilever at the same time as the topographic image. SR-MFM images of alternating magnetic fields diverging from the main pole in a driving perpendicular magnetic recording head are presented, and the divergence and convergence of the fields are discussed. The spatial resolution of SR-MFM is estimated to be 18 nm; this is 2.5 times smaller than that of conventional MFM. © 2012 American Institute of Physics. [<http://dx.doi.org/10.1063/1.4705400>]

### I. INTRODUCTION

Magnetic imaging and analysis techniques have contributed to the development of magnetic recording media such as hard disk drives.<sup>1–5</sup> Magnetic force microscopy (MFM) is one of the most widely used scanning probe microscopy (SPM) techniques for imaging the stray magnetic field distribution with a high lateral resolution of approximately 10 nm in a static magnetic field.<sup>2,6</sup> Some studies have reported improvements to MFM techniques for measuring static magnetic fields,<sup>1</sup> however, few have focused on developing MFM techniques for detecting an alternating magnetic field. One technique reported for this purpose is high-frequency MFM (HF-MFM);<sup>7–9</sup> however, its resolution is not comparable to that of conventional MFM in a static magnetic field.<sup>10</sup> Currently, in the area of magnetic recording media, there is a strong need not only to miniaturize the recording bits but also to increase the recording speed, because of which stray magnetic fields change dynamically. Therefore, techniques for detecting an alternating magnetic field with high spatial resolution are of great importance. Recently, Saito *et al.*<sup>11–13</sup> reported the frequency modulation MFM (FM-MFM) technique and showed that it could achieve a spatial resolution of 15 nm. In FM-MFM, the first resonant frequency of the cantilever vibration  $f_1$  is modulated by the alternating magnetic field with frequency  $f_m$ , and magnetic signals are obtained using a heterodyne method with a modulated frequency of  $f_1 - f_m$ . After acquiring the topographic signal by the first raster scan, the magnetic signal is obtained by successive raster scans with a small lift of the cantilever from the surface. In principle, because FM-MFM uses frequency modulation of the first resonant frequency  $f_1$  for obtaining magnetic images, a surface roughness can also modulate  $f_1$  and thus interfere with the magnetic images. One solution for reducing this interference is to apply a phase-lock loop (PLL) circuit to maintain a constant frequency difference of  $f_1 - f_m$ .<sup>12,13</sup> Another solution is to obtain the magnetic images using not  $f_1$  but another resonant frequency such as the second resonant frequency. Recently, Venstra *et al.* demonstrated Q-factor con-

trol of a cantilever by mechanical sideband excitation at the sum ( $f_1 + f_2$ ) and difference ( $f_1 - f_2$ ) frequencies.<sup>14</sup> Although the coupling between  $f_1$  and  $f_2$  flexural modes appears at the sum and difference frequencies, the interferences between  $f_1$  and  $f_2$  do not appear at  $f_1$  and  $f_2$  frequencies themselves.

In this study, we develop secondary resonance MFM (SR-MFM) for imaging alternating magnetic fields from a sample surface. Our technique simultaneously measures the secondary resonant frequency of the magnetic cantilever and obtains the topographic image. In SR-MFM, as the alternating magnetic field signals are detected by the second resonant frequency of the cantilever, the topographic signals that originate from the first resonant mode do not interfere with the alternating magnetic field signals even if the cantilever is close to the sample surface (within a few nanometers). We demonstrate the driving current dependence of the SR-MFM images on the perpendicular magnetic recording head, and we discuss the spatial resolution of SR-MFM.

### II. EXPERIMENTAL

A schematic diagram of the SR-MFM system is shown in Fig. 1(a). SR-MFM images were observed using a modified MFM (SII, SPA300HV), and a ferromagnetic cantilever was employed (Nanoworld Point Probe Plus MFMR, coercivity: 300 Oe). This cantilever was oscillated by applying an external voltage with a driving frequency of  $f_d = 67.346$  kHz. Topographic images were obtained with a peak-to-peak vibration amplitude of 64 nm<sub>p-p</sub>.

Figures 1(b) and 1(c) show the amplitude of the cantilever as a function of frequency. The first  $f_1$  and second  $f_2$  resonant frequencies of the cantilever are estimated to be  $f_1 = 67.474$  and  $f_2 = 424.324$  kHz, respectively. The vibration of the cantilever without any loaded force is theoretically described by considering elastic vibration.<sup>15</sup> Accordingly,  $f_1$  and  $f_2$  are given as follows:

$$f_1 = \frac{1}{2\pi} \times 3.5160 \sqrt{\frac{EI}{mL^4}}, \quad (1)$$

$$f_2 = \frac{1}{2\pi} \times 22.0345 \sqrt{\frac{EI}{mL^4}}, \quad (2)$$

<sup>a)</sup>Author to whom correspondence should be addressed. Electronic mail: majima@msl.titech.ac.jp.

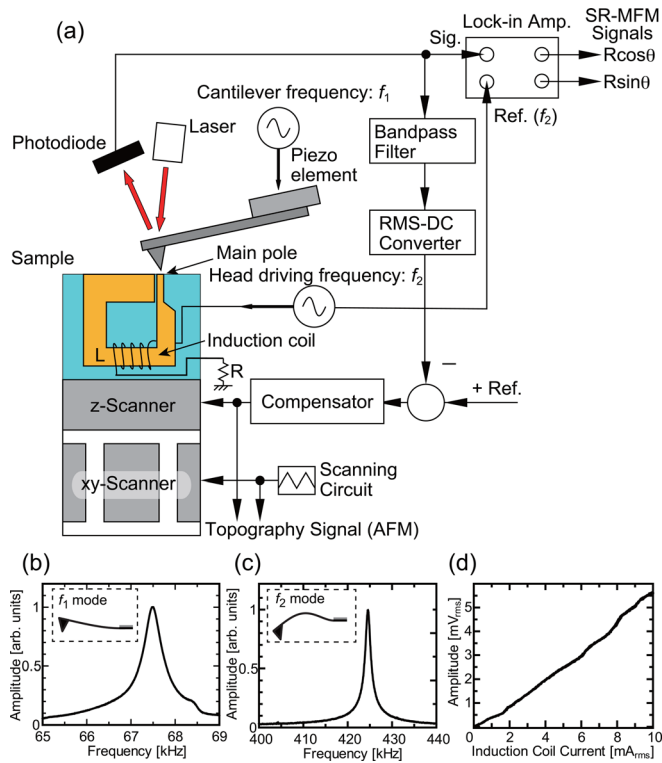


FIG. 1. (a) Schematic diagram of the SR-MFM system. Frequency spectrum of the cantilever vibration around (b) the first resonant frequency  $f_1$  and (c) the second resonant frequency  $f_2$ . Insets show a schematic illustration of the vibration mode. (d) Dependence of the SR-MFM amplitude  $R$  on the induction coil current of the perpendicular magnetic recording head.

where  $E$  is the modulus of elasticity;  $I$  is the cross-sectional area moment of inertia about an axis perpendicular to the longitudinal direction of the cantilever;  $m$  is the mass per unit length along the longitudinal direction of the cantilever; and  $L$  is the length of the cantilever. According to this theory, the cantilever vibrates easily not only at  $f_1$  but also at  $f_2$ . Note that the experimental frequency ratio  $f_2/f_1$  is 6.29, which is close to the theoretical ratio of 6.27.

A single-pole perpendicular magnetic recording head is driven by applying a sinusoidal current to the induction coil. Alternating magnetic fields whose frequencies are the same as that of the sinusoidal current diverge from the main pole. When the frequency of the sinusoidal current is set to  $f_2$ , the ferromagnetic cantilever vibrates because of the magnetic force at  $f_2$ . Figure 1(d) shows the dependence of the cantilever amplitude on the induction coil current at resonant frequency  $f_2$  under superimposed cantilever vibration at  $f_1$  by the cantilever piezo. The vibration amplitude was measured by using a lock-in amplifier (Stanford Research, SR844)

with a reference signal of  $f_2$  when the cantilever is placed on the main pole of the head. In Fig. 1(d), the amplitude is almost proportional to the current, indicating that the alternating magnetic field from the main pole is proportional to the induction coil current and that the amplitude at  $f_2$  can be measured even with the existence of ensemble vibrations of  $f_1$  and  $f_2$ . These results allow us to measure the alternating magnetic field by using the  $f_2$  component independently of the cantilever vibration amplitude.

Two scans were taken at the same line to obtain the topographic and magnetic signals as follows. The topographic signal was obtained by the first scan by using  $f_1$  with a cantilever amplitude of 71.4 nm<sub>p-p</sub> (the so-called tapping mode). The magnetic signal was obtained by the second scan by using  $f_2$  with a cantilever amplitude of 17.4 nm<sub>p-p</sub>, while maintaining 1-nm separation between the sample surface and the minimum position of the vibrating cantilever using the topographic information acquired in the first scan. The cantilever vibration signals were detected by using a photodiode. The absolute values of the peak-to-peak amplitude of the oscillations at  $f_1$  and  $f_2$  were determined by the amplitude signals  $R$  of lock-in amplifier signals measured at  $f_1$  and  $f_2$ , respectively. The alternating magnetic force (SR-MFM signal) was measured as  $R \cos \theta$  and  $R \sin \theta$  signals by the lock-in amplifier at  $f_2$ , where  $R$  and  $\theta$  are the amplitude and phase difference of the reference signal, respectively. The phase difference  $\theta$  was set to zero immediately before the second scan. During the second scan, the vibration amplitude of the  $f_2$  component was less than 1 nm<sub>p-p</sub> at an induction coil current of 20 mA<sub>rms</sub>. In the conventional MFM technique, the cantilever has to be lifted to a few tens of nanometers in order to prevent interference of the topographic information with the magnetic information, because both signals are detected by the  $f_1$  signal. All measurements were carried out in ambient conditions at room temperature. We note that a small lift of 1 nm is a feature of SR-MFM, which enables us to observe a magnetic image with high spatial resolution without the interference of the topographic information due to the adoption of the different resonant frequencies, that is,  $f_2$  and  $f_1$ .

### III. RESULTS AND DISCUSSION

Figures 2(a) and 2(b) show the topographic image and SR-MFM amplitude signal  $R$  (where  $R = \sqrt{(R \cos \theta)^2 + (R \sin \theta)^2}$ ) of the perpendicular magnetic recording head at an induction coil current and frequency of 1 mA<sub>rms</sub> and  $f_2 = 424.324$  kHz, respectively. The perpendicular magnetic recording head consists of a wedge-shaped main

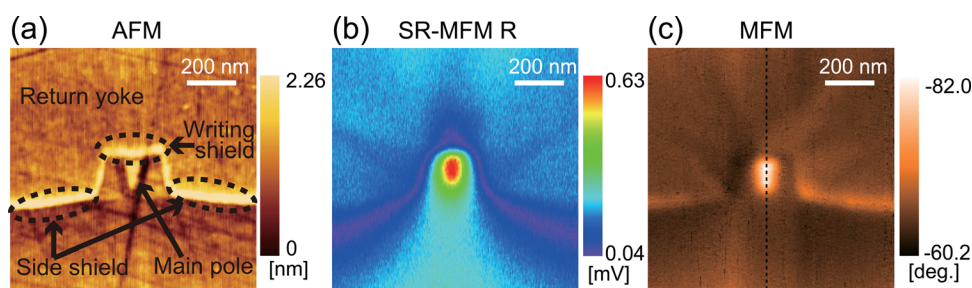


FIG. 2. (a) Topographic image and (b) SR-MFM amplitude  $R$  image of the perpendicular magnetic recording head under an induction coil current and frequency of 1 mA<sub>rms</sub> and  $f_2 = 424.324$  kHz, respectively. (c) Conventional MFM image of the same perpendicular magnetic recording head with an induction coil dc of 5 mA.

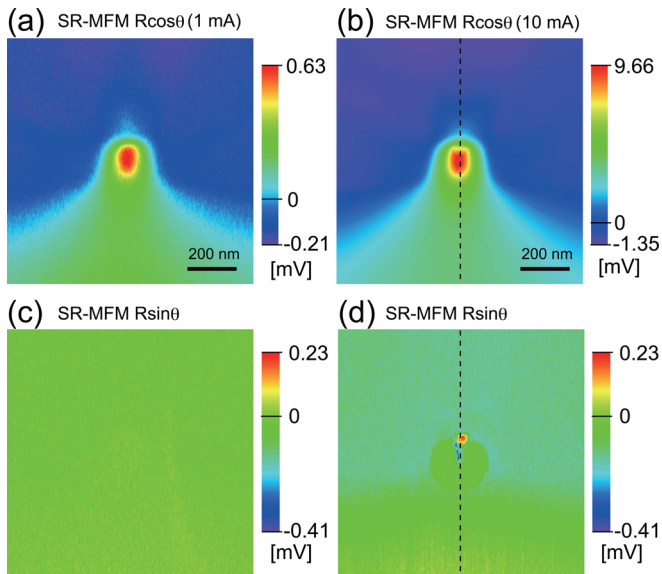


FIG. 3. SR-MFM  $R \cos \theta$  images for an induction coil current of (a) 1 and (b) 10 mA<sub>rms</sub>. The simultaneously observed SR-MFM  $R \sin \theta$  images are shown in (c) and (d).

pole, a writing shield, a side shield, and a return yoke; all these features were observed in the topographic image. The distance between the main pole and the writing shield was 20 nm. As shown in Fig. 2(b), the magnetic field amplitude is maximum at the main pole.

Figure 2(c) shows a conventional MFM image of the same perpendicular magnetic recording head taken with the same cantilever at an induction coil dc of 5 mA. As the main pole is bright in the image, a repulsive force is observed on the main pole. As a result, the static magnetic field is lesser than the coercivity of the cantilever under a dc of 5 mA; in other words, the magnetization direction of the cantilever does not change during MFM image observation. A comparison of Figs. 2(b) and 2(c) shows that the spot size of the main pole in the SR-MFM  $R$  image is smaller than that in the conventional MFM image.

Figures 3(a) and 3(b) show SR-MFM  $R \cos \theta$  images for induction coil currents of 1 and 10 mA<sub>rms</sub>, respectively, and Figs. 3(c) and 3(d) show the corresponding  $R \sin \theta$  images that were observed simultaneously. In Figs. 3(a) and 3(b), the largest  $R \cos \theta$  signal is observed at the main pole, as in the case of the  $R$  image in Fig. 2(b). Because there is no recording medium with a soft magnetic layer, the magnetic flux from the main pole is substantially reduced. The  $R \cos \theta$

signals at the main pole and return yoke show a positive and negative value, respectively, especially in the 10 mA<sub>rms</sub> image, indicating that the magnetic flux diverges from the main pole and converges at the return yoke. Therefore, SR-MFM  $R \cos \theta$  images reveal information about not only the alternating magnetic field amplitude but also the magnetic field direction.

The phase  $\theta$  of the magnetic force and the induction coil current were set to zero before the magnetic image observation. In the  $R \sin \theta$  images of Figs. 3(c) and 3(d), the  $R \sin \theta$  signal was zero over the entire area for a current of 1 mA<sub>rms</sub>, while there was a clear signal at the main pole for a current of 10 mA<sub>rms</sub>. When the magnitude of the alternating magnetic field originating from the main pole is less than the coercivity of the cantilever, the magnetization of the cantilever does not change and a flat  $R \sin \theta$  image is observed (Fig. 3(c)). As a result, the direction of the magnetic force applied to the cantilever changes while the same phase of the alternating magnetic field due to the induction coil current at a frequency of  $f_2$  is maintained.

In contrast, when the amplitude of the alternating magnetic field becomes larger than the coercivity of the cantilever, the magnetization direction of the cantilever is inverted at the phase for which the magnetization direction is opposite to that of the magnetic field, and the magnetic force of the cantilever changes from repulsive to attractive, because the magnetization directions are parallel. The change in the force direction results in a cantilever vibration phase shift, and the phase difference  $\theta$  is no longer zero, as observed in Fig. 3(d). Therefore, the bright spot in the  $R \sin \theta$  image indicates the region where the magnetic field exceeds the coercivity of the cantilever, 300 Oe. Note that the signal spot size of the main pole in Fig. 3(d) is not only smaller than that in Fig. 3(b) but is also smaller than that observed in the topographic image shown in Fig. 2(a). Consequently, we can observe a magnetic image using the  $R \sin \theta$  signal when the magnetic field is larger than the coercivity.

Figures 4(a) and 4(b) show the spatial resolutions of the SR-MFM  $R \cos \theta$  and  $R \sin \theta$  images obtained from Fourier transformations of the line profiles in Figs. 3(b) and 3(d), respectively. When the spatial resolution is defined by the inverse of the critical frequency at which the power spectrum intensity is less than the thermal background noise, it can be estimated by the cross point between the extrapolated downward slope line and the flat line that shows the thermal background noise, as shown in Fig. 4.<sup>13,16</sup> In Figs. 4(a) and 4(b),

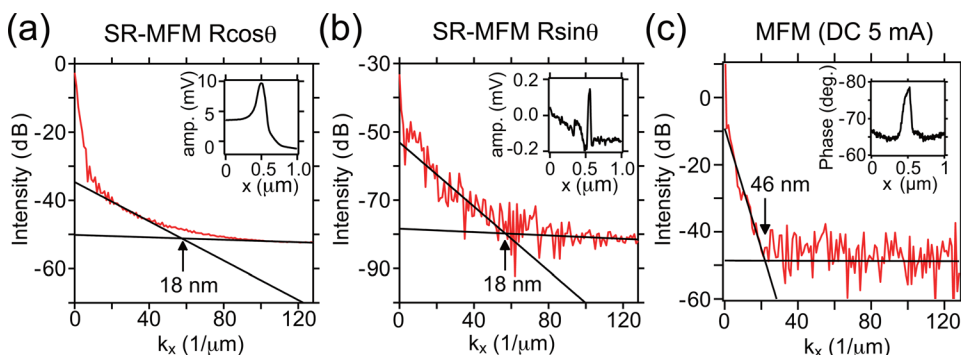


FIG. 4. Fourier transform of the (a)  $R \cos \theta$ , (b)  $R \sin \theta$ , and (c) conventional MFM line profiles taken along the lines indicated in Figs. 3(a), 3(b), and 2(c), respectively. The line profiles are shown in the insets.

the spatial resolution of both the  $R \cos \theta$  and  $R \sin \theta$  images is evaluated to be 18 nm. We note that the spatial resolution is similar to that of FM-MFM, as reported by Lu *et al.*<sup>13</sup> Figure 4(c) shows the spatial resolution of conventional MFM images under a direct current of 5 mA obtained from a Fourier transformation of the line profile shown in Fig. 2(c). The spatial resolution is evaluated to be 46 nm. Consequently, the spatial resolution of SR-MFM is 2.5 times smaller than that of conventional MFM for the same perpendicular recording head driven by a direct current with the same magnetic cantilever.

#### IV. CONCLUSION

In this study, we have developed SR-MFM, in which the alternating magnetic field image is detected by the second resonant vibration signal of the cantilever at the same time as the topographic image. The SR-MFM  $R \cos \theta$  image includes information about the direction as well as the amplitude of the alternating magnetic field. SR-MFM  $R \sin \theta$  imaging enables us to clarify the position at which the alternating magnetic field exceeds the coercivity of the cantilever. The spatial resolution of SR-MFM is estimated to be 18 nm; this is 2.5 times smaller than that of conventional MFM for the same perpendicular recording head driven by a direct current with the same magnetic cantilever. The SR-MFM technique is thus quite promising for developing a perpendicular magnetic recording head with high spatial resolution.

#### ACKNOWLEDGMENTS

We would like to thank Dr. Katsuaki Yanagiuchi, TDK Corp., for supplying the perpendicular magnetic recording head. This study was partially supported by a Grant-in-Aid

for Scientific Research on Innovative Areas (No. 20108011,  $\pi$ -Space) from the Ministry of Education, Culture, Sports, Science and Technology (MEXT), Japan; the Global COE Program of “Photonics Integration-Core Electronics,” MEXT; the Collaborative Research Project of Materials and Structures Laboratory, Tokyo Institute of Technology; and the World Class University (WCU) Program through the Ministry of Education, Science and Technology of Korea (R31-10022).

- <sup>1</sup>Y. Martin and H. K. Wickramasinghe, *Appl. Phys. Lett.* **50**, 1455 (1987).
- <sup>2</sup>D. Rugar, H. J. Mamin, P. Guethner, S. E. Lambert, J. E. Stern, I. McFadyen, and T. Yogi, *J. Appl. Phys.* **68**, 1169 (1990).
- <sup>3</sup>A. Hubert and R. Schäfer, *Magnetic Domains: The Analysis and Magnetic Microstructures* (Springer, Berlin, 2000).
- <sup>4</sup>A. Okuda, J. Ichihara, and Y. Majima, *Appl. Phys. Lett.* **81**, 2872 (2002).
- <sup>5</sup>S. Suzuki, Y. Azuma, and Y. Majima, *Appl. Phys. Lett.* **90**, 053110 (2007).
- <sup>6</sup>P. Grütter, Th. Jung, H. Heinzelmann, A. Wadas, E. Meyer, H.-R. Hidber, and H.-J. Güntherodt, *J. Appl. Phys.* **67**, 1437 (1990).
- <sup>7</sup>R. Proksch, P. Neilson, S. Austvold, and J. J. Schmidt, *Appl. Phys. Lett.* **74**, 1308 (1999).
- <sup>8</sup>M. Abe and Y. Tanaka, *IEEE Trans. Magn.* **38**, 45 (2002).
- <sup>9</sup>M. R. Koblischka, J. D. Wei, and U. Hartmann, *J. Phys.: Conf. Ser.* **61**, 591 (2007).
- <sup>10</sup>M. R. Koblischka, M. Kirsch, R. Pfeifer, S. Getlawi, F. Rigato, J. Fontcuberta, T. Sulzbach, and U. Hartmann, *J. Magn. Magn. Mater.* **322**, 1697 (2010).
- <sup>11</sup>H. Saito, H. Ikeya, G. Egawa, S. Ishio, and S. Yoshimura, *J. Appl. Phys.* **105**, 07D524 (2009).
- <sup>12</sup>H. Saito, W. Lu, K. Hatakeyama, G. Egawa, and S. Yoshimura, *J. Appl. Phys.* **107**, 09D309 (2010).
- <sup>13</sup>W. Lu, Z. Li, K. Hatakeyama, G. Egawa, S. Yoshimura, and H. Saito, *Appl. Phys. Lett.* **96**, 143104 (2010).
- <sup>14</sup>W. J. Venstra, H. J. R. Westra, and H. S. J. van der Zant, *Appl. Phys. Lett.* **99**, 151904 (2011).
- <sup>15</sup>L. Meirovitch, *Fundamentals of Vibrations* (McGraw-Hill, New York, 2000), p. 401.
- <sup>16</sup>H. Hopster and H. P. Oepen, *Magnetic Microscopy of Nanostructures* (Springer, Berlin, 2003).